PERGAMON

Vision Research 39 (1999) 3934–3950

Vision Research

www.elsevier.com/locate/visres

The variation of torsion with vergence and elevation

J. Porrill [a], J.P. Ivins [b,*], J.P. Frisby [a]

[a] *Department of Psychology, University of Sheffield, Western Bank, Sheffield S10 2TN, UK*
[b] *Department of Computer Science, Curtin University of Technology, GPO Box U1987, Perth 6845, Western Australia*

Received 24 July 1998; received in revised form 2 February 1999

Abstract

Two recently developed kinematic models of human eye movements predict systematic departures from Listing's law which are associated with changes in vergence. This vergence-dependent torsion t is proportional to elevation e and vergence v, that is $t = kev/2$. The proposed value for k is either 1 (Van Rijn, L. J., & Van den Berg, A. V. (1993). *Vision Research*, *33*, 691–708) or 1/2 (Minken, A. W. H., Gielen, C. C. A. M., & Van Gisbergen, J. A. M. (1995). *Vision Research*, *35*, 93–102). One implication of both models is that an eye with a constant fixation direction should exhibit systematic torsional variation during movements of the other eye. This paper therefore examines the torsion produced by moving a fixation target inwards and outwards along the line-of-sight of the right eye at five different viewing elevations (0, ± 15 and $\pm 30°$). In a monocular analysis, each eye generally showed intorsion during convergence at positive elevation angles, whereas extorsion occurred at negative elevations; the opposite was true during divergence. However, the torsion response was visibly different between the five subjects, and depended on the direction of target motion. In a binocular analysis, cycloversion (mean of left and right eye torsion) varied dramatically both between subjects and between convergence and divergence; however, cyclovergence (torsional difference) was much less variable. Least-squares methods were used to estimate the constant k from monocular torsion, yielding values between 0.2 and 1.0; however, corresponding estimates based on cyclovergence were all close to 1/2. These findings support suggestions that a binocular control system couples the three-dimensional movements of the eyes, and that an existing model of monocular torsion should be generalised to the binocular case.

Keywords: Cyclotorsion (torsion); Cyclovergence; Cycloversion; Eye movements; Listing's law; Vergence; Vertical horopter

1. Introduction

The human eye has three rotational degrees of freedom: in addition to the horizontal and vertical movements which direct it to the fixation point, the eye can also rotate about its line-of-sight; this behaviour is called cyclotorsion (torsion). Hence, in theory, an infinite number of distinct eye orientations are compatible with each fixation direction. In practice, however, in the absence of head tilt and with static visual surroundings the amount of torsion shown by the eye, measured relative to any system of axes, is (roughly) determined by its horizontal and vertical orientation about these axes. The eye therefore appears to use only two of its three rotational degrees of freedom; this observation is known as Donders' law.

A refinement of Donders' law known as Listing's law specifies the amount of torsion for a given fixation direction (Helmholtz, 1867). From any initial orientation, the eye assumes only those orientations that can be reached by rotations about axes that lie in a single plane. This plane is called the displacement plane, and the different planes associated with different initial orientations do not coincide. There is one particular displacement plane to which the initial fixation direction is orthogonal; this plane is called Listing's plane, and with the head upright the associated primary fixation direction is roughly straight ahead.

As yet there is no generally accepted explanation for Listing's law; furthermore, random and systematic deviations from this law arise from the following sources (in addition to those produced by the vestibular system):

- Seemingly random fluctuations in torsion over a range of approximately $\pm 0.5°$ which occur continu-

* Corresponding author.
E-mail address: ivinsj@cs.curtin.edu.au (J.P. Ivins)

0042-6989/99/$ - see front matter
PII: S0042-6989(99)00102-9

ously even during fixation on static targets (Enright, 1990).
- Torsional hysteresis between fixations on the same point (Enright, 1990).
- Vergence-dependent torsion, which is equivalent to rotation of Listing's plane during vergence as reported in several recent studies—for example, see Mok, Ro, Cadera, Crawford and Vilis (1992).
- Individual differences (Bruno & Van den Berg, 1997).

Ivins, Porrill and Frisby (1999) examined all these sources of torsional variation during smooth asymmetric vergence changes at a viewing elevation of $+15°$. Torsion did not vary significantly between trials of the experiment, or between experimental sessions; however, torsion did depend on the direction of vergence change (convergence or divergence), and there were obvious differences between subjects. Torsion of the two eyes could be divided into stable cyclovergence and unstable cycloversion—only cyclovergence was accurately controlled in dynamic conditions.[1] There were idiosyncratic differences in monocular torsion and cycloversion patterns during convergence and divergence; however, inter-subject differences in cyclovergence were almost negligible. Furthermore, the differences were reproducible in different trials and sessions of the experiment.

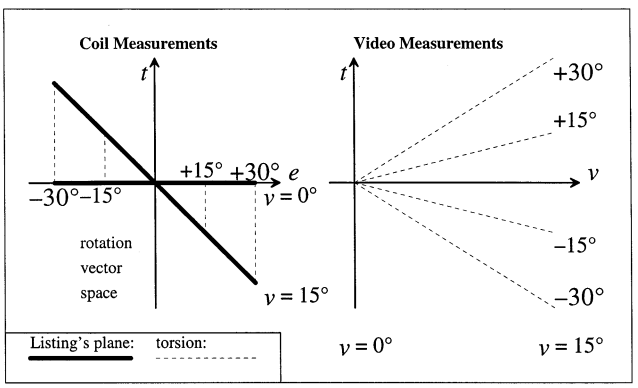

Fig. 1. Representing eye orientation. This diagram shows the relationship between scleral coil measurements of Listing's plane during constant vergence (as reported in previous studies), and measurements of torsion t during asymmetric vergence changes (as reported in this study). For both sets of measurements torsion changes (dashed lines) are shown for five different angles of elevation e. (LHS) For coil measurements Listing's plane in the right eye is shown viewed from above (thick lines), at two angles of vergence $v = 0$ and 15°. (RHS) It is not possible to plot Listing's plane using measurements from the video system, partly because there is no common zero to act as a reference when combining multiple trials, and partly because the angle of vergence is changing and hence Listing's plane is rotating continually. Instead the eye-tracking system measures torsion relative to Fick co-ordinates, with the convention that intorsion is positive.

[1] Binocular torsion can be described in terms of *cycloversion* (half the sum), and *cyclovergence* (half the difference) computed from left and right eye torsion.

This paper is mainly concerned with vergence-dependent deviations from Listing's law; however, other sources of torsion are examined where appropriate, since a complete explanation of torsional eye movements must incorporate all such components.

1.1. Vergence-dependent torsion

Listing's law is generally obeyed during version when the fixation axes of the two eyes are roughly parallel (distant viewing). During vergence, however, the relationship between fixation direction and torsion alters, producing an outward rotation of Listing's plane for each eye as shown in Fig. 1 (LHS); this saloon door swing pattern is associated with changes in torsion—see Tweed (1997).

Two kinematic models of human eye movements attempt to predict the systematic torsional departures from Listing's law which arise during changes in vergence. Given angles of elevation e and vergence v measured in radians, the predicted torsion relative to that specified by Listing's law is:

$$t \approx k\frac{ev}{2} \tag{1}$$

Van Rijn and Van den Berg (1993) obtained data which suggest that $k = 1$; Minken, Gielen and Van Gisbergen (1995) argue that $k = 1/2$ based on data from Mok et al. (1992). These models clearly do not obey Donders' law since the torsional state of each eye is not determined solely by its monocular fixation direction; however, they each amount to a binocular extension of Listing's law in which the torsional state of each eye is completely determined by the fixation point. (The extended laws reduce to the original form when the vergence or elevation angle is zero.)

Despite their differences, one implication of both kinematic models is that an eye with a constant fixation direction can exhibit systematic torsional variation associated with changes in vergence due to movements of the other eye—as when fixating different points along the same line-of-sight. This prediction was confirmed in the asymmetric vergence experiment reported by Ivins et al. (1999); however, the study only examined torsion at a single viewing elevation.

1.2. Asymmetric vergence

The asymmetric vergence task was previously described by Nakayama (1983). A subject was placed in a head restraint and asked to fixate a succession of points at decreasing depths along the line-of-sight of the right eye. A series of photographs of this eye were subsequently compared to a reference photograph using a

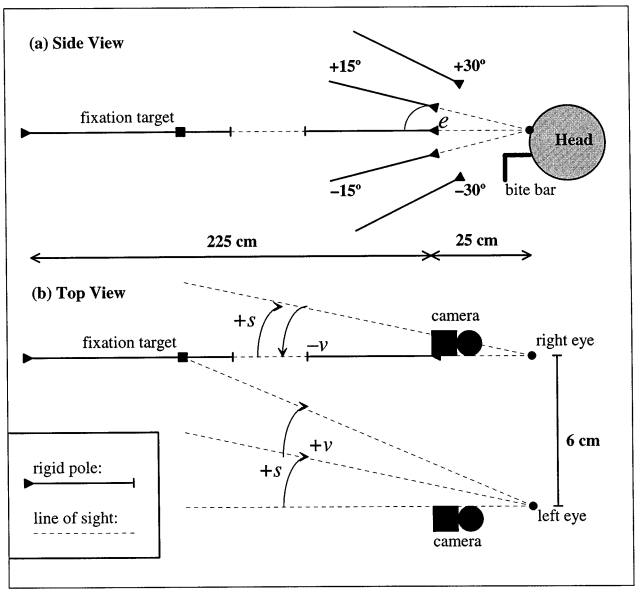

Fig. 2. Apparatus and eye geometry during asymmetric vergence. This diagram shows two views of the apparatus used to measure the variation of torsion during asymmetric vergence (not to scale). The human subject was immobilised by a bite bar near which two video cameras were mounted—one for each eye. A rigid pole projected between the cameras from a depth of 25–250 cm. A fixation target was moved along the pole, which was aligned with one of five possible lines-of-sight for the right eye at 0, ± 15 or $\pm 30°$ elevation. During asymmetric vergence the (identical) version s and vergence v angles combine in the mobile left eye, but cancel out in the immobile right eye.

manual alignment procedure to estimate torsion. (This experiment is a direct test of Listing's law since the horizontal and vertical orientation of the right eye is fixed, while the left eye is free to move to maintain binocular fixation.) The asymmetric vergence task was repeated at elevation angles of 0 and $\pm 20°$.[2] The results suggested that, for a particular fixation direction, the torsional state of the eye depended on the amount of vergence and elevation; however, the exact form of this dependence was not clear.

The experiment described by Nakayama (1983) suffers from at least three deficiencies. First, measurements were made using a small number of photographs which apparently come from just one subject (the description of the method is not clear on this point). Second, the study did not allow for the variations in monocular torsion which occur during fixation on immobile targets—see Enright (1990) and Ivins, Porrill and Frisby (1998). Third, torsion was only measured in the fixed right eye, not in the mobile left eye. There is clearly a need to replicate this experiment to eliminate these deficiencies.

[2] Note that 0° elevation implies a horizontal line-of-sight with the head upright.

1.3. Aims and overview

This paper describes an extension of the experiment reported by Nakayama (1983) designed to measure the variation of torsion with asymmetric vergence and elevation, and to improve on the original experiment in the following ways:

- Five subjects were used to investigate individual differences; each subject took part in multiple trials of the experiment.
- Eye movements were measured using a video eye-tracking system to analyse image sequences automatically, rather than taking measurements by hand from a small number of photographs.
- Torsion was measured independently from both eyes of each subject, allowing binocular data analysis and interpretation.
- The asymmetric vergence task was modified to involve fixation on a moving target; this allowed for a simple investigation of hysteresis using inward (to subject) versus outward (from subject) target motion.

The remainder of this paper examines monocular and binocular torsion during smooth asymmetric convergence and divergence with the right eye fixating at 0, ± 15 and $\pm 30°$ elevation.

2. Methods

Further information regarding the subjects and apparatus is given by Ivins et al. (1999).

2.1. Subjects

There were five subjects, all males aged between 21 and 39; a complete orthoptic examination was performed on each. Four subjects (JP, PD, PW and SH) had normal visual acuity. The other subject (JI) had excellent near acuity at 1/3 m but reduced far acuity at 6 m (6/12 instead of 6/6) which improved to normal with refractive correction. (The correction was not present during the experiment because spectacles and contact lenses interfere with the process of measuring eye movements from video images.) Otherwise, all five subjects were within normal limits for orthoptic examinations, with good stereo acuity (60 s of arc or better), good ocular alignment, and good muscle control.

2.2. Apparatus

The apparatus shown in Fig. 2 was based on a metal frame bolted to the floor and walls of the laboratory to minimise vibration and other movements. The frame enclosed a rigid pole, each end of which was mounted on a sturdy adjustable tripod, allowing it to be carefully aligned with the line-of-sight of the right eye at differ-

Table 1
Experimental design[a]

Elevation	+30°		+15°		0°		−15°		−30°	
Motion	In	Out	In	Out	In	Out	In	Out	In	Out
JI/JP/PW	×5	×5	×5	×5	×5	×5	×5	×5	×5	×5
PD/SH	×5	×5	×5	×5	×5	×5	×5	×5		

[a] The torsion response of five subjects was measured at four or five different viewing elevations; at each elevation a fixation target was moved five times alternately inwards and outwards along the line-of-sight of the right eye.

ent elevations. A mobile fixation target consisting of a black cross on a white rectangle 3 cm square was mounted on the pole. All components except the target were painted black, and the entire frame was covered in black cloth to eliminate external light, giving almost complete control over viewing conditions.

The subject was immobilised in the apparatus using a customised bite bar coated with dental plastic in which an impression of the teeth was made. The head was kept upright by placing the forehead on a headrest while biting on the dental mould. Vergence-dependent torsion was studied by asking the subject to fixate on the target as it moved in depth along the rigid pole between 25 and 250 cm. The target was driven at constant velocity by a stepper motor and pulley system, covering the 225 cm in 15 s.

2.3. Design

Movements of the right and left eyes of each subject were recorded during asymmetric vergence changes at five different viewing elevations (0, ±15 and ±30°). However, measurements for the −30° case could not be obtained from two of the subjects (PD and SH) because their eyelids obscured their irises. A single experimental trial involved exposing a subject to one continuous movement of the fixation target inwards or outwards along the line-of-sight of the right eye at a single elevation. (The right eye held a constant fixation direction throughout each trial, whereas the left eye moved to maintain binocular fusion.)

During each trial approximately five pairs of images (one for each eye) were saved every second for off-line analysis. Each trial lasted approximately 15 s, and trials were performed in groups of ten, alternating between inward and outward motion, with a gap of approximately 15 s between trials to allow the subject to rest and blink. This design, which is summarised in Table 1, yielded two (eyes) × five (trials) × two (directions) = 20 image sequences per elevation from each subject. In all there were 23 groups of trials or 460 sequences in all, each containing 70–80 images. The total recording time was therefore about 1 h, yielding approximately 36 000 images and hence torsion measurements.

Image sequences for each elevation were collected on separate days to avoid fatigue and boredom in the subjects. To minimise learning effects the order of presentation of the elevations was different for each subject; however, such effects seem very unlikely given that Ivins et al. (1999) found no differences between equivalent measurements obtained under identical conditions on different days.

2.4. Measuring torsion from video images

For every trial of the experiment measurements were made of horizontal and vertical eye orientation, torsion, and pupil size. Video images were analysed off-line using the eye-tracking system developed by Ivins et al. (1998). This system performs correlation of band-pass filtered, transformed iris sectors to recover torsion—see Moore, Haslwanter, Curthoys and Smith (1996). Unlike other systems, however, it uses a low-parameter deformable model of the iris. As a result, the new system can deal with pupil expansion and contraction, and therefore avoids the need to constrict the iris with drugs. The system has been tested extensively, and is accurate to within 0.1° for torsion measurements.

The data analyses assume that torsion is related to fixation distance (vergence), and hence to target distance; however, these distances might be rather different from each other. To eliminate this possibility measurements of horizontal and vertical eye orientation were used to assess whether or not subjects were always fixating the target accurately. None of the experimental trials revealed any evidence to suggest that subjects were not fixating on the moving targets. (The left eye exhibits a great deal of horizontal movement to produce the required vergence, accompanied by a very small vertical movement which is most obvious during near convergence; the right eye remains stationary in all trials.) Hence it appears that fixation distance and target distance are essentially equivalent in the present context.

Changes in torsion were measured relative to a Fick frame—see Haslwanter (1995)—as illustrated in Fig. 1 (RHS), with the convention that positive rotations were clockwise in the image, representing intorsion in the right eye and extorsion in the left.[3] (Measurements

[3] The direction of a change in monocular torsion is specified using the upper pole of the vertical meridian of the iris—rotation of this pole inwards (medially) is called *intorsion*; rotation outwards (laterally) is called *extorsion*.

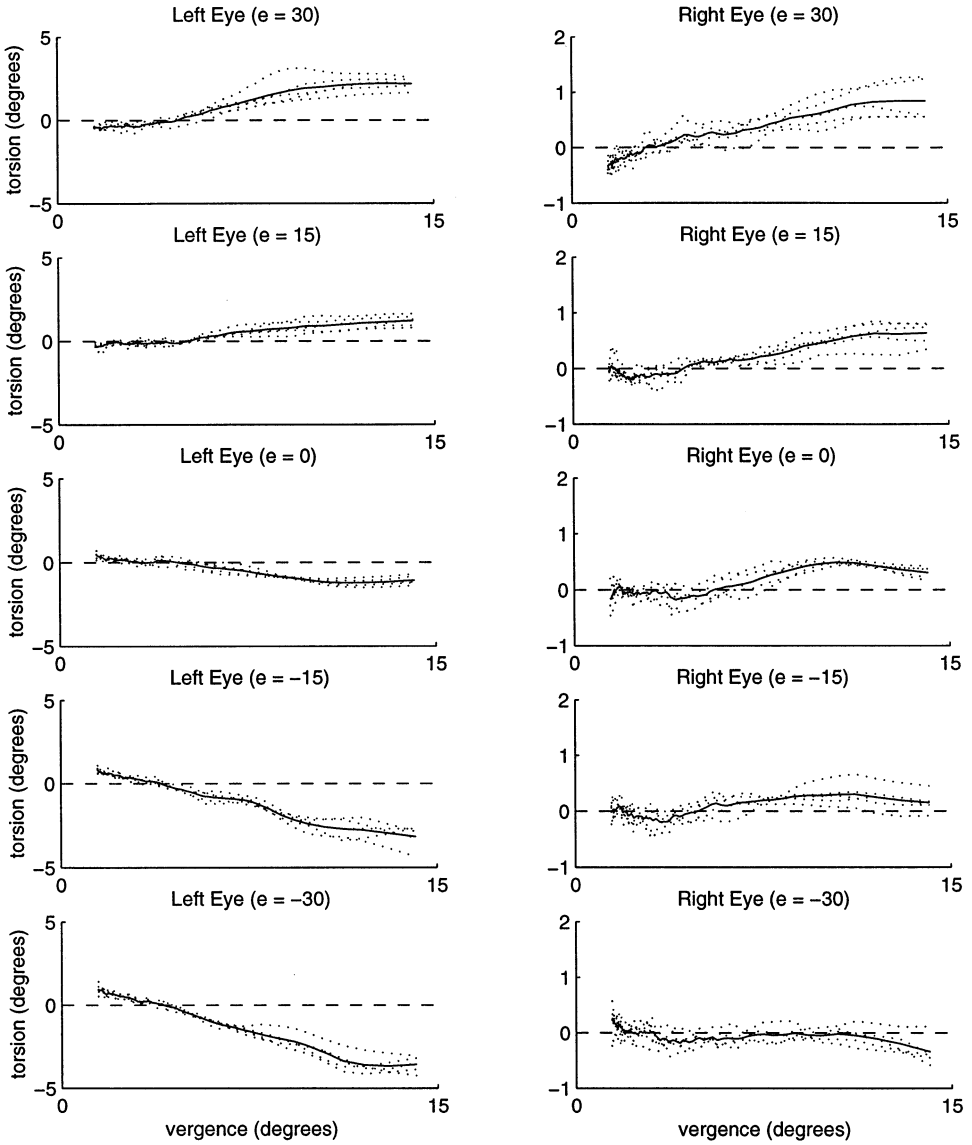

Fig. 3. Torsion during individual trials of asymmetric vergence. These graphs show torsion measurements from one subject (JP) during inward motion of the fixation target along the line-of-sight of the right eye at five different elevations (0, ± 15 and $\pm 30°$). Torsion is plotted as a function of vergence, rather than fixation distance (time). Note the difference between the ordinate scales for the left and right eyes. Each graph shows results from five independent trials (dotted lines); the mean of each set of five trials (solid lines) is also shown. Measurements from the left eye have been negated so that, for both eyes, positive rotation is intorsion and negative rotation is extorsion.

from the left eye are sometimes negated for graphical purposes; however, the correct interpretation is specified in the appropriate figure captions.) It is not possible to obtain accurate plots of Listing's plane from these measurements, because vergence is continually changing and hence the plane is continually rotating as illustrated in Fig. 1 (LHS).

3. Results

The results of each trial were independently normalised by subtracting the mean torsion computed over the trial. This was necessary because eye movements within each trial were measured relative to the first image from the corresponding video sequence, making it impossible to know the absolute state of the eye—hence only changes in torsion could be measured.

Example measurements from individual trials of convergence (inward target motion) are shown for one subject (JP) in Fig. 3. Torsion patterns from trials performed under identical conditions are very similar. However, small (apparently random) fluctuations occur continuously over a range of $\pm 0.5°$. This noise was eliminated by computing mean torsion measurements for each set of five trials (convergence or divergence). Mean monocular and binocular results from all five subjects are described in the next two subsections.

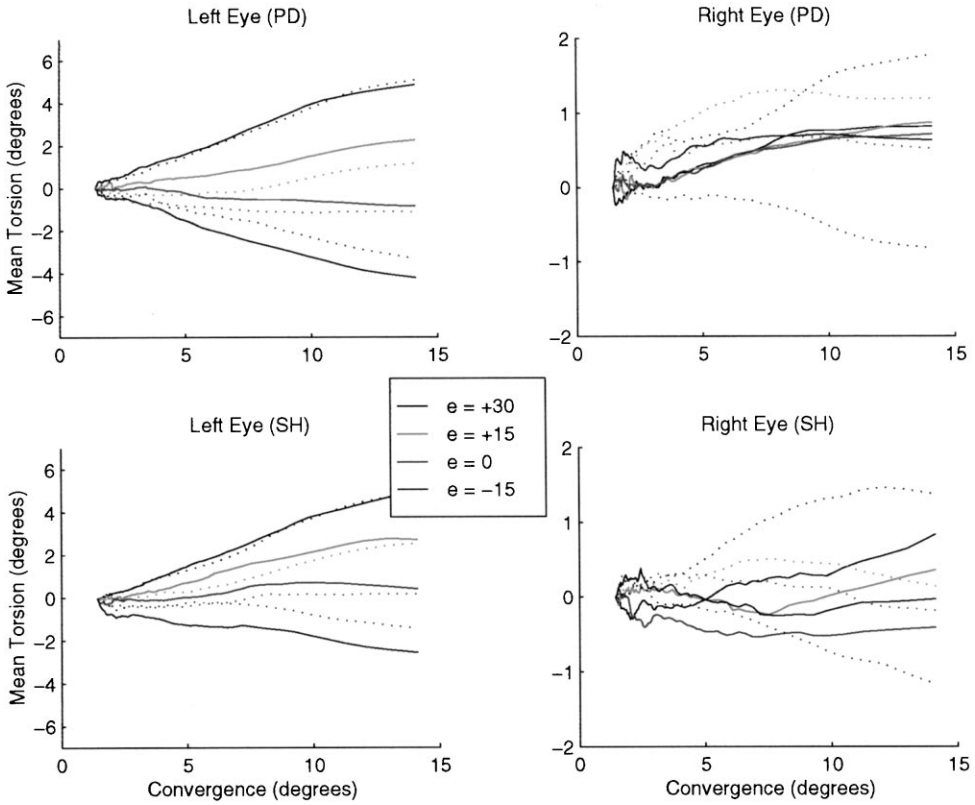

Fig. 4. Monocular variation of torsion with vergence and elevation. These graphs show the variation of torsion with vergence measured at four different elevations; results are shown for two subjects (PD and SH), whose eyelids obscured their irises in the $-30°$ viewing condition. Results for inward target motion are shown using solid lines; dotted lines indicate outward motion. In all cases intorsion is positive; extorsion is negative. The left eye graphs show a trend from intorsion to extorsion with decreasing elevation; however, this trend is not present in all of the right eye graphs.

Torsion of the left and right eyes is plotted as a function of vergence angle, as opposed to fixation (target) distance, with the right eye at each of five elevations[4]. This format is necessary for calculating the k values which are the main focus of the experiment. Measurements obtained from near fixations are thus more numerous than those obtained at far fixations; however, this bias is instructive since most torsion occurs during near fixation. Ivins et al. (1999) describe an extensive analysis of torsion in terms of fixation distance.

3.1. Mean monocular torsion (by subject)

Figs. 4 and 5 summarise the variation of torsion with vergence and elevation for all five subjects; mean results (over five trials) are shown for both inward and outward target motion. In nearly all graphs there is a trend from intorsion during increasing vergence at positive elevations to extorsion at negative elevations. For comparison, Fig. 10 in the Appendix shows the torsion patterns predicted using Listing's law and the kinematic models of vergence-dependent torsion.

As expected, torsion magnitude is much smaller for the immobile right eye than for the mobile right eye, which shows up to 5° of systematic torsion as it moves to maintain fixation on the target. Nevertheless, the right eye clearly violates Listing's law by exhibiting up to 2° of torsion, the exact form of which varies between subjects according to the direction of target motion. The results show a clear relationship between torsion and vergence which becomes more pronounced as elevation increases; however, this is not always symmetric about the 0° (horizontal) elevation. The torsion-free elevation—the elevation at which no overall change in monocular torsion occurs during vergence—is therefore different for each subject. In other words, the right eye shows an idiosyncratic asymmetric deviation from Listing's law, with a bias towards intorsion in some subjects and extorsion in others. A corresponding binocular analysis (Section 3.2) suggests that this effect is not an experimental artefact.

[4] The horizontal component of Fick vergence was computed from fixation (target) distance d as $\tan^{-1}(I/d)$ where the interocular separation I (in mm) for each subject was JI = 63, JP = 66, PD = 63, PW = 57 and SH = 62, giving a mean of 62.2. This expression is a lowest-order approximation to the more usual Helmholtz vergence, and has adequate accuracy in the experimental situation (see Section A.3).

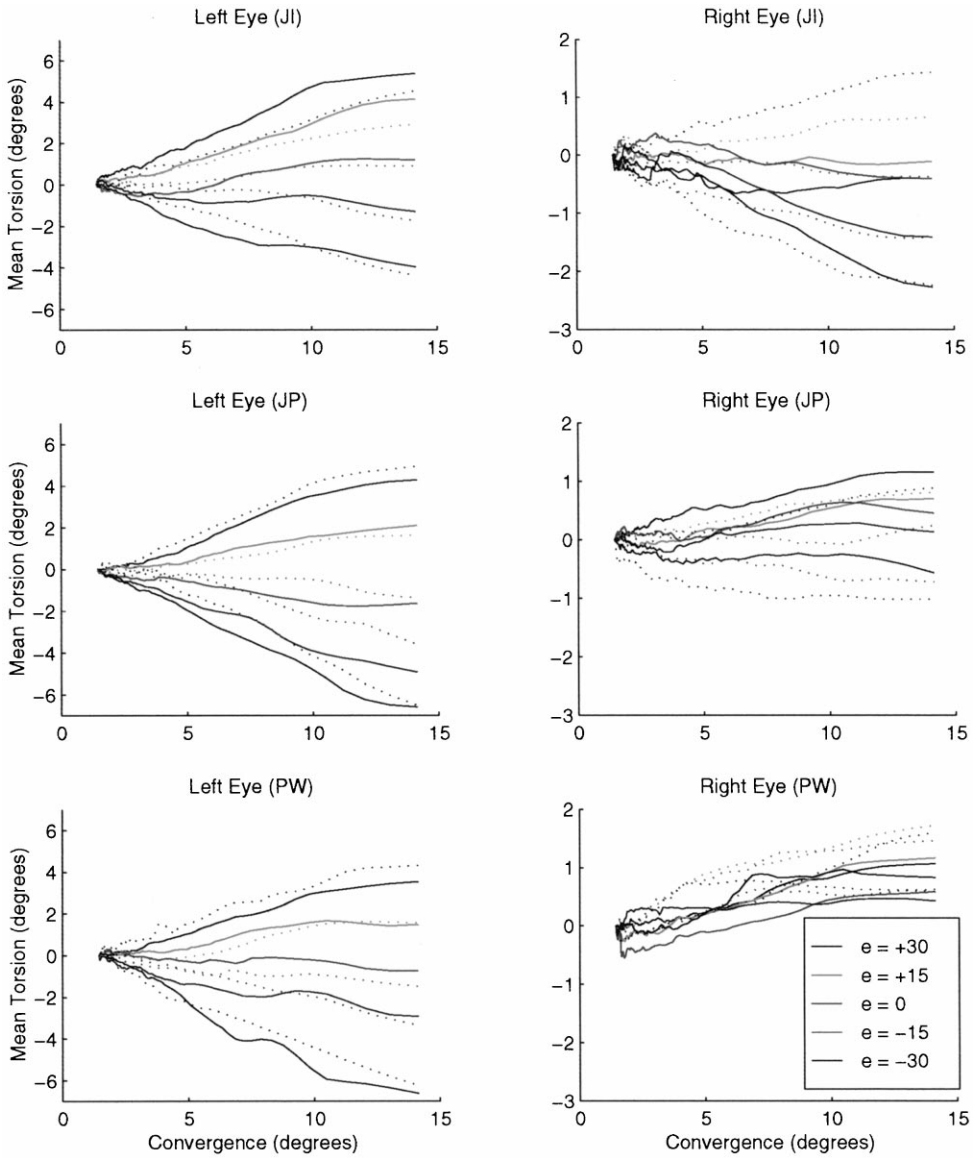

Fig. 5. Monocular variation of torsion with vergence and elevation. These graphs show the variation of torsion with vergence measured at five different elevations; results are shown for three subjects (JI, JP and PW). Results for inward target motion are shown using solid lines; dotted lines indicate outward motion. In all cases intorsion is positive; extorsion is negative. The left eye graphs show a trend from intorsion to extorsion with decreasing elevation; however, this trend is not present in all of the right eye graphs.

The torsion patterns are visibly different between the five subjects in Figs. 4 and 5; in addition, the patterns are different for inwards versus outwards target motion. For example, JI shows no overall right eye torsion at 15 and 30° elevation during inward target motion; however, during outward motion only the 0° (horizontal) elevation fails to produce torsion. The other four subjects exhibit comparably idiosyncratic torsion patterns. Ivins et al. (1999) showed that the idiosyncratic differences and apparent hysteresis are not simply due to random variation, and can be replicated in trials performed several weeks apart.

3.2. Mean binocular torsion (by subject)

Corresponding torsion measurements from the left and right eyes can be decomposed into binocular cycloversion and cyclovergence. Cycloversion, S, is computed as the mean of the left L and right R eye rotation so that $S=(L+R)/2$, with positive values indicating an overall clockwise shift (in the video image); negative values indicate an anticlockwise shift. Cyclovergence, G, is computed as half the difference between the rotation of the two eyes so that $G=(L-R)/2$, with positive values indicating an overall

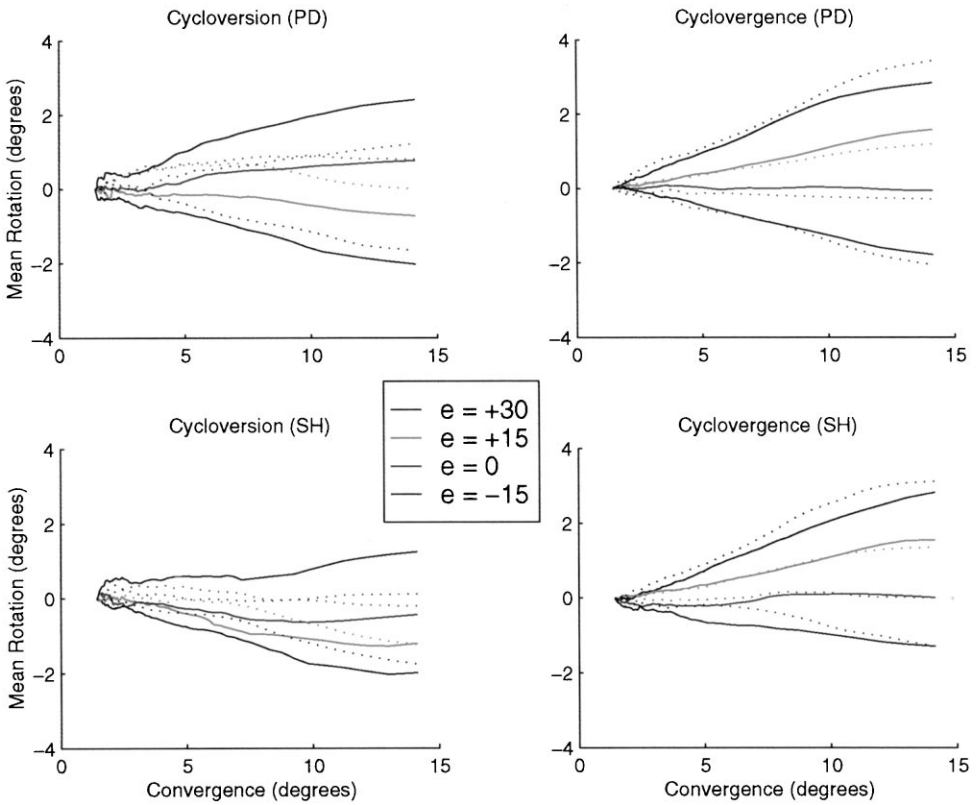

Fig. 6. Binocular variation of torsion with vergence and elevation. These graphs show binocular torsion from two subjects (PD and SH). Each graph shows mean results from groups of five trials of asymmetric vergence performed at each of four angles of right eye elevation. Results for inward target motion (convergence) are shown as solid lines; outward motion (divergence) is indicated with dotted lines.

relative intorsion; negative values indicate relative extorsion.

Figs. 6 and 7 show binocular torsion based on the monocular data from Figs. 4 and 5. Cycloversion varies dramatically both between subjects and according to the direction of target motion. However, this is not the case for cyclovergence, which is much more stable and less noisy; graphs for cyclovergence are similar for all five subjects, regardless of the direction of motion.

In contrast to the monocular torsion patterns shown in Figs. 4 and 5, all five subjects show roughly no change in cyclovergence at 0° (horizontal) elevation. Thus the variation in monocular torsion at 0° elevation appears to reflect idiosyncratic cycloversion changes, rather than misalignment of the fixation target or deviation of the head away from upright.

3.3. Modelling vergence-dependent torsion

The mean results were used to calculate the gradient of torsion against vergence at each elevation, yielding estimates of the disputed k value from the models of vergence-dependent torsion proposed by Van Rijn and Van den Berg (1993) and Minken et al. (1995). Appendix A gives formulae for the left and right eye torsion, and cycloversion and cyclovergence predicted by these kinematic models for the asymmetric vergence paradigm. Both models predict a linear relationship between torsion and vergence for constant viewing elevation. A linear least-squares fit can therefore be used to estimate the constant k from Eq. (1) using the torsion measurements from the experiment, and hence indicate which of the models is most accurate.

3.3.1. Method

The formulae relating torsion y to the product of vergence and (constant) elevation ev (all angles in radians) have linear forms as follows:

$$y = m\,ev + c \tag{2}$$

Specific linear formulae for left and right eye torsion, and for cyclovergence can be obtained from Eq. (A.8) or Table 4 in Appendix A; cycloversion does not depend on the k value in either of the kinematic models, and so cannot be used for least-squares fitting.

A least-squares fit was used to find the coefficients m and c in Eq. (2) using the mean torsion data for each subject; the gradient m was subsequently used to find estimates of k for the various data sets via the formulae in Table 2. The offset parameter c is ignored since torsion is always measured relative to the first image in

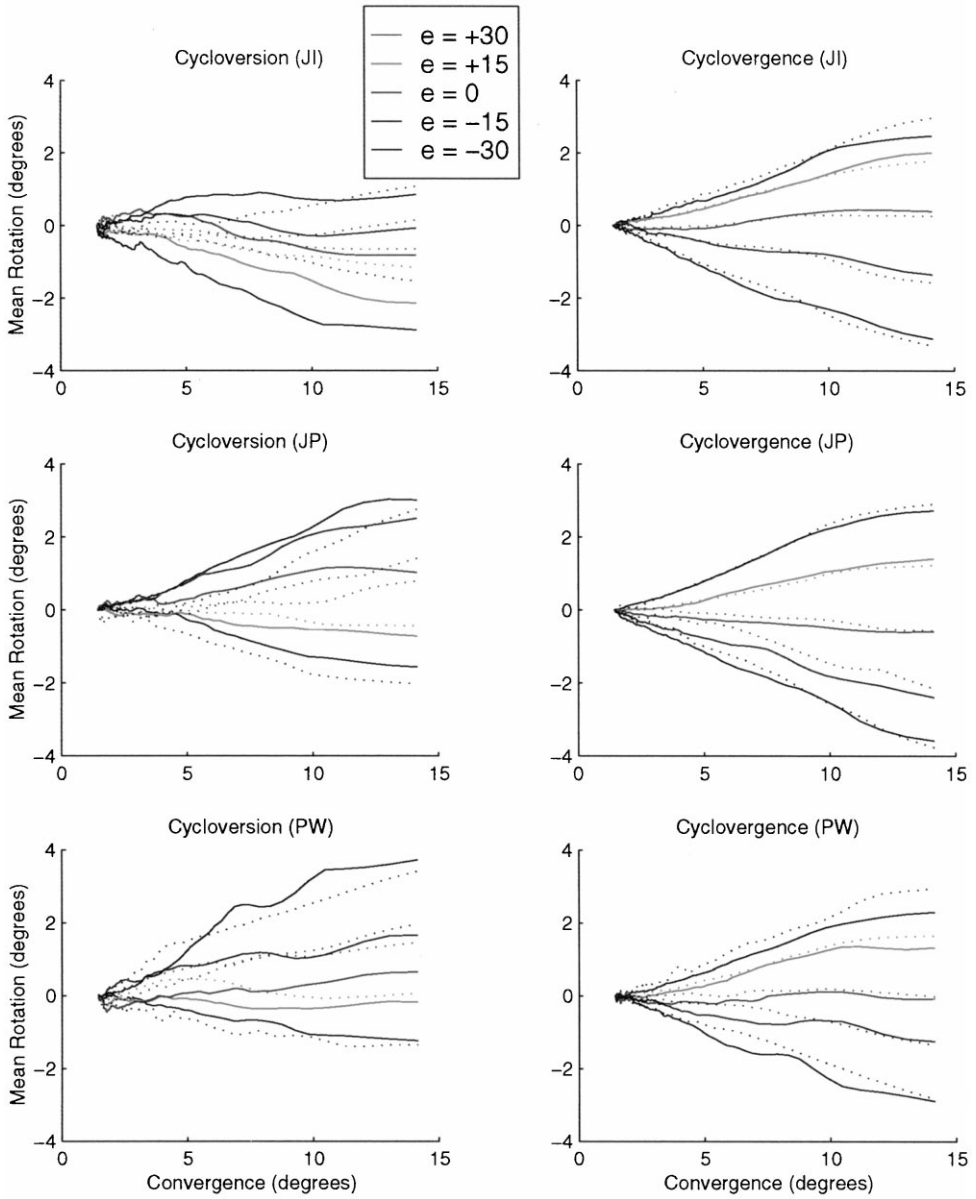

Fig. 7. Binocular variation of torsion with vergence and elevation. These graphs show binocular torsion from three subjects (JI, JP and PW). Each graph shows mean results from groups of five trials of asymmetric vergence performed at each of five angles of right eye elevation. Results for inward target motion (convergence) are shown as solid lines; outward motion (divergence) is indicated with dotted lines.

sequence; consequently, this parameter contains no useful information.

3.3.2. Results

The results of estimating k using the mean data (Figs. 4–7) for each of the five subjects are summarised in Table 3 and Fig. 8. Measurements obtained at 0° (horizontal) elevation cannot be used since *ev* is then zero; this is consistent with the fact that both kinematic models assume there is no vergence-dependent torsion without elevation (though this is clearly not the case in Figs. 4 and 5). The range of values from the least-squares fit was 0.21–1.03 for the mobile left eye, 0.16–0.65 for the immobile right eye, and 0.38–0.61 for cyclovergence.

Comparisons of left eye ($t = 3.72$, $P = 0.021$ with four dof) and right eye ($t = -4.24$, $P = 0.013$) estimates revealed significant differences in monocular torsion between convergence and divergence. However, there was no significant difference between the estimates obtained using the corresponding cyclovergence ($t = 0.82$, $P = 0.457$ with four dof). A non-parametric analysis gave equivalent results.

3.4. Summary

Torsion of the left and right eyes is shown in Figs. 4 and 5. As in several previous studies, during increasing vergence both eyes generally showed intorsion at positive

Table 2
Least-squares parameters[a]

Torsion	Formula from Appendix A	y	m	k
Left eye	$L=\frac{(k+1)}{2}ev+c$	L	$\frac{k+1}{2}$	$2m-1$
Right eye	$R=-\frac{k}{2}ev+c$	R	$-\frac{k}{2}$	$-2m$
Cyclovergence	$L=-\left(\frac{2k-1}{4}\right)ev+c$	G	$-\left(\frac{2k-1}{4}\right)$	$\frac{1-4m}{2}$

[a] This table shows the components of the least-squares formulae for approximating the measured torsion L and R in the left and right eyes, and the corresponding cyclovergence G.

elevations, and extorsion at negative elevations; the opposite was true during decreasing vergence. The magnitude of the torsion response was much larger for the mobile left eye than for the otherwise immobile right eye (which did not rotate horizontally or vertically). Both eyes showed continuous, seemingly random torsional fluctuations over a range of about $\pm 0.5°$. In addition, there were differences between convergence (inward motion) and divergence (outward motion)—each eye showed hysteresis in that, for any given elevation and vergence angles, the torsional state depended on previous eye movements. Monocular torsion patterns were also visibly different between subjects.

A further analysis in terms of binocular torsion is shown in Figs. 6 and 7. Cycloversion varied considerably between subjects and showed significant dependence on the direction in which the fixation target was moving. Cyclovergence was much more stable and less noisy than cycloversion, and did not appear to depend on the direction of motion; it merely depended on the position of the fixation target. Both hysteresis (differences between convergence and divergence) and differences between subjects were much less apparent in cyclovergence than in cycloversion.

Estimates of k computed from mean monocular torsion vary between 0.2 and 1.0 depending on the subject and the direction of vergence change; in contrast, corr-

Table 3
Gradient of torsion against vergence and (constant) elevation[a]

Motion	Left eye torsion		Right eye torsion		Cyclovergence	
	In	Out	In	Out	In	Out
JI	0.640	0.420	0.350	0.610	0.490	0.510
JP	1.030	0.640	0.190	0.410	0.610	0.520
PD	0.850	0.360	0.220	0.650	0.530	0.510
PW	0.650	0.630	0.160	0.220	0.410	0.420
SH	0.590	0.210	0.190	0.540	0.390	0.380
Mean	0.752	0.452	0.222	0.486	0.486	0.468

[a] This table shows the values of k for each subject. Estimates obtained using measurements from the left and right eyes are very variable, both between subjects and between directions of target motion (in and out), and clearly reflect the variability of monocular torsion. However, estimates obtained from the cyclovergence data are much more uniform at around 1/2 for both inward and outward target motion, and these estimates are consistent between subjects.

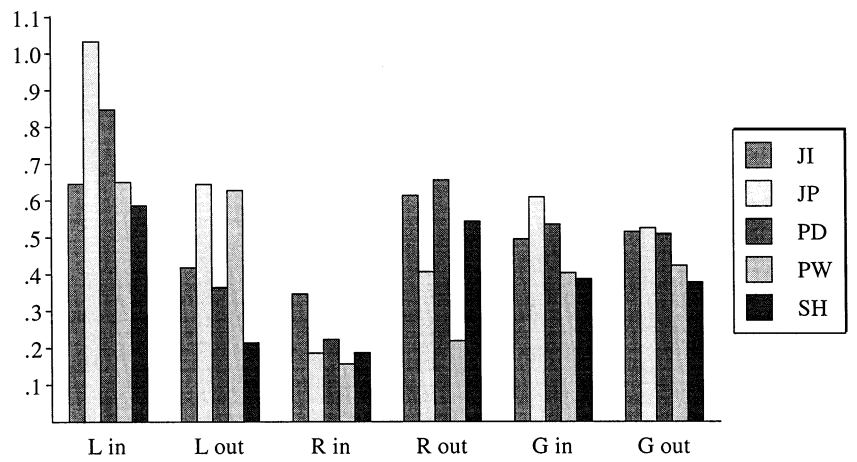

Fig. 8. Mean gradient estimates during convergence and divergence. This chart shows the mean estimates of the k value for the left L and right R eyes and for cyclovergence G computed for each subject. Estimates from left and right eye torsion show considerable variation, both between subjects and between in and out conditions; in contrast, estimates from cyclovergence are much more consistent, with values close to 1/2.

sponding estimates from cyclovergence suggest a value of about 0.5.

4. Discussion

The variation of monocular and binocular torsion during smooth asymmetric vergence at different elevations can be summarised as follows: cyclovergence is stable and depends on where the two eyes are looking, whereas cycloversion (and hence monocular torsion) is unstable and depends on how they came to be in the current horizontal and vertical state. Most of the monocular variation in torsion can be accounted for by changes in cycloversion (or vice-versa). These findings reinforce suggestions that the binocular torsional state of the eyes is more important than the state of the left and right eyes individually, and that relative torsional movements of the two eyes are coupled.

The results appear to reflect the use of separate neural control strategies for cycloversion and cyclovergence. Presumably these strategies serve one or more useful purposes such as minimising (or at least stabilising) the disparity along the horizontal meridians, or tilting the vertical horopter in an appropriate way. Control of cycloversion is not nearly so crucial to stereo vision as is accurate maintenance of cyclovergence, which is important for the metric interpretation of stereo disparities. Furthermore, cyclovergence determines the slant of the vertical horopter and thus the working volume for stereo. Better control of cyclovergence could thus be required for maintenance of stereo constancy.

4.1. Comparison with previous experiments

Nakayama (1983) reported that there was no systematic change in the torsional state of the fixed right eye for upward ($+20°$) elevation, even though the vergence angle increased from about 3 to 25°; however, for horizontal and downward ($-20°$) elevation the right eye showed 3° of extorsion as the angle of vergence increased. These results differ from those of the present study which found systematic intorsion at positive elevations, and extorsion at negative elevations. This discrepancy may be explained by the fact that only a small amount of data was gathered in the original experiment, using a laborious and potentially inaccurate manual technique to measure torsion from photographs. It was therefore not possible to examine differences in torsion between subjects, or to allow for the instability of monocular torsion during fixation. Furthermore, measurements were only taken from the right eye, so the study did not examine cycloversion or cyclovergence.

The results of this experiment agree with those from previous experiments involving static fixations and saccades in at least three important ways.

- There were obvious (apparently random) variations in the monocular torsion shown by each subject over about $\pm 0.5°$; Enright (1990) reported similar variations during fixation on static targets.
- The mean cycloversion patterns obtained from each set of five trials, though repeatable between experimental sessions as demonstrated by Ivins et al. (1999), showed variations between inward and outward tracking conditions. In other words, there was hysteresis such that cycloversion (and monocular torsion) depended on previous eye movements—see Enright (1990).
- There were obvious differences between the mean cycloversion (and monocular torsion) patterns shown by different subjects—see Bruno and Van den Berg (1997).

A combination of these effects, particularly the individual differences and hysteresis seen in Table 3 and Fig. 8, may explain the discrepancies between the experimental estimates of the constant k reported by Van Rijn and Van den Berg (1993) and Minken et al. (1995). Neither of the corresponding kinematic models capture the range or types of variation in monocular torsion shown by different subjects during smooth asymmetric vergence. Despite this monocular variation, however, binocular cyclovergence is consistent with a value of $k = 1/2$ for all subjects. Hence, although the results do not support a binocular extension to Listing's law as suggested by the kinematic models, they do support a weaker form of Listing's law: the relative torsional state (cyclovergence) of the two eyes is determined by binocular fixation.

4.2. Explanations for Listing's law and vergence-dependent torsion

Several hypotheses have been advanced regarding the purpose of Listing's law and its vergence-dependent deviations, the main categories of which are briefly outlined below.

4.2.1. Mathematical elegance

Listing's law effectively reduces the number of degrees of freedom for ocular rotation, from three to two; thus the constraints imposed by it might simplify the eye muscle control law. However, there are many other ways of doing this—Listing's law is just one special case of Donders' law. A complete explanation must identify the specific advantages of the chosen strategy.

4.2.2. Biophysical optimisation

Listing's law might arise as a consequence (side-effect) of ocular mechanics. The oldest theory of this type, put forward by Fick and Wundt (see Helmholtz,

1867), holds that Listing's law enhances motor efficiency by minimising the rotational eccentricity of the eye; a modern mathematical formulation is given by Hepp (1990). Minimising eye rotation away from some rest state minimises the exertion required to maintain an eccentric orientation, and allows fast and accurate responses to oculomotor stimuli. Several minor objections can be made to this theory—for example, it assumes that eye movements obeying Listing's law require the least effort, which is uncertain. However, the major flaw in the theory is that it cannot explain vergence-dependent departures from Listing's law.

4.2.3. Functionality

Perhaps the most important hypothesis is that Listing's law offers some functional advantage. For example, Hering (1868) noted that eye movements obeying Listing's law preserve direction congruence for lines passing through the primary fixation direction.[5] Helmholtz (1867) proposed a similar hypothesis—that Listing's law could optimise certain aspects of image flow across the retina, thereby simplifying the neural processing of visual information. Unfortunately, these two theories are no better than the biophysical explanations at explaining vergence-dependent torsion.

A complete explanation for torsion might combine all three of the above elements. Whatever their functional explanation, if Listing's law and vergence-dependent torsion are important then evolution will presumably have adapted the human eye and its muscle system to be biophysically optimal for implementing these strategies, at least to within some tolerance. (Biophysical optimisation is highly dependent on function—after all, the simplest least effort strategy is not to move the eyes at all!) Likewise, if a function has important symmetry then the resulting implementation is likely to be mathematically interesting.

A preliminary attempt at unifying these theories is described by Tweed (1997) who suggests that a strategy which combines the function of stereo vision with biophysical (motor) constraints might explain Listing's law and vergence-dependent torsion. The proposed visual-motor strategy attempts to accomodate two conflicting aims—aligning the images of the visual plane, and minimising ocular eccentricity—which uniquely determine the orientation of both eyes. This strategy does not ensure single vision of lines orthogonal to the visual plane, but rather reduces cyclodisparity of the visual plane itself.

[5] If a straight line is viewed so that it intersects the primary direction then the orientation-sensitive cells which are best tuned for this line will also be the best tuned cells at other fixation directions that intersect the line.

4.3. The vertical horopter

The horopter consists of those points in space having binocular correspondence; it is defined as the locus of all points in the visual field, the images of which fall upon corresponding points on the two retinas. Assuming a geometric model of retinal correspondence, the vertical portion of the horopter is a vertical line through the fixation point, at least for symmetric vergence in the horizontal plane. In practice, however, the empirical horopter is tilted backward and passes through the feet of a subject viewing targets at infinity (Helmholtz, 1867). This tilt is a consequence of the deviation from strict geometric correspondence between the two retinas, producing a physiological shear of the vertical meridian in each eye. As a result, for eyes with parallel horizontal fixation axes (viewing distant targets straight ahead) the horopter line lies approximately in the groundplane—a useful place for depth discrimination to be optimal. Assuming no violations of Listing's law, during symmetric convergence the horopter orientation becomes closer and closer to vertical.

Nakayama (1983) suggested that Listing's law might be important in controlling binocular correspondence during non-parallel fixation, and that vergence-dependent deviations from Listing's law might give the vertical horopter a functionally appropriate tilt for the close viewing associated with convergence. In this scenario, a small advantage might be obtained by extorsion during convergence because it tilts the horopter backwards slightly. This additional tilt during near fixation might aid in the binocular inspection of backward tilted surfaces. To the extent that such surfaces receive better illumination from overhead sources (presumably the sun) compared to most vertical surfaces, they will be well placed to ensure optimal binocular stimulation.

Fig. 9 shows the orientation of the horopter line for varying distances of symmetric fixation at different elevations, predicted using measurements from the smooth asymmetric vergence task. These predictions are different from those of Nakayama (1983) since the they are based on a partly conflicting set of measurements. There are three main sources of relative torsion (cyclovergence) and hence horopter tilt:

- The built-in relative shear ψ_H of the vertical meridians of the two eyes originally hypothesised by Helmholtz (1867) which cannot be measured using eye-tracking techniques; this is equivalent to 2° of extorsion according to Tyler (1983), while Nakayama (1983) gives a value of 1.5°.
- Torsion ψ_L due to Listing's law in accordance with Eq. (A.5) in Appendix A.
- Vergence-dependent (roughly antisymmetric) torsion t possibly in accordance with one of the two kinematic models described in Section 1; Table 3 suggests that $k = 1/2$ for cyclovergence.

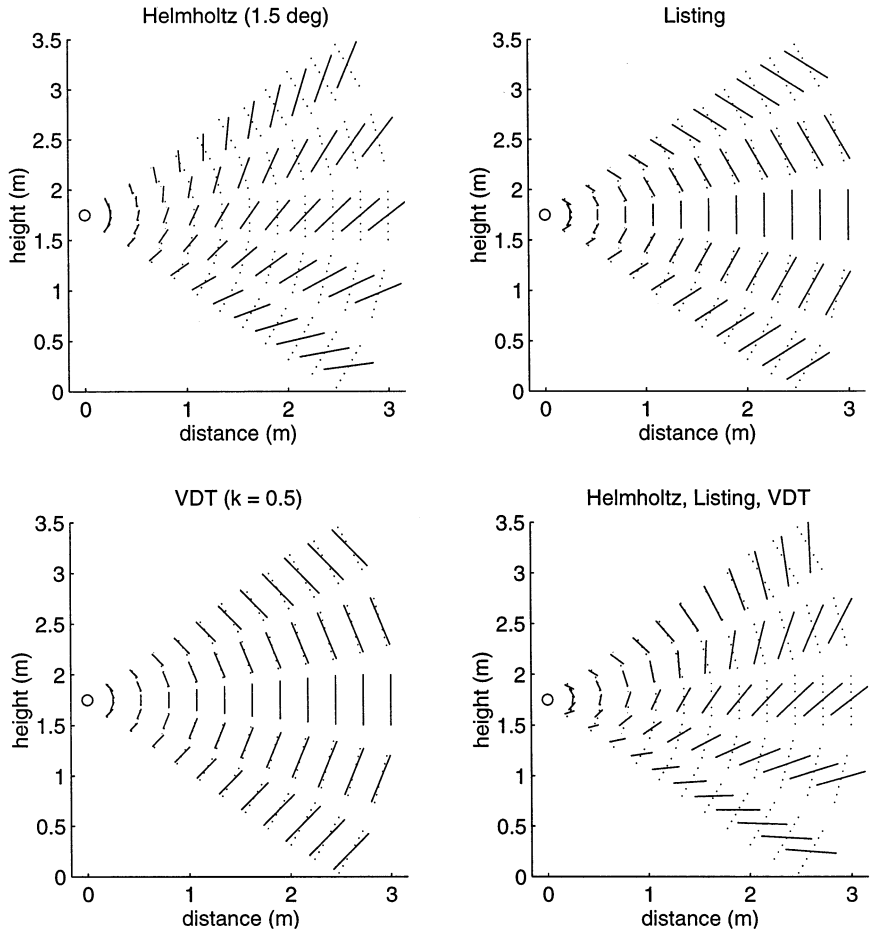

Fig. 9. Orientation of the vertical horopter. These diagrams show the predicted orientation of the vertical horopter line for symmetric vergence at each of five elevations (0, ± 15 and $\pm 30°$). Horopter orientation is calculated from estimates of ψ_H, ψ_L and t (black lines); the orientation of the horopter without these effects is also shown (dotted lines). Top-left shows the tilt produced by the physiological torsion ψ_H of the two retinae relative to each other; this is grossly asymmetric about the horizontal. Top-right shows the tilt produced by torsion ψ_L due to Listing's law; this is symmetric about the horizontal. Bottom-left shows the effect of vergence-dependent torsion t ($k = 1/2$), which is also symmetric. Bottom-right show the combined effect of all three sources of torsion. The horopter line lies in the groundplane during downward gaze, and is approximately vertical during upward gaze; however, vergence-dependent torsion has very little impact on overall horopter orientation.

A small advantage might be obtained from the vergence-dependent cyclovergence seen in Figs. 6 and 7 because it tilts the horopter backward slightly during convergence at negative elevations (downward fixation); however, it also tilts the horopter forward slightly during convergence at positive elevations (upward fixation). Furthermore, both these effects are very small compared with the Helmholtz and Listing contributions, which suggests that vertical horopter placement is unlikely to be the functional motivation for vergence-dependent torsion.

5. Conclusions

There are many possible monocular implementations of Donders' law, of which Fick and Helmholtz motion are two examples; however, Listing motion more closely resembles the strategy used by the human visual system and is thus presumably (almost) optimal according to some biological criteria yet to be determined. Extensions of Listing's law for predicting vergence-dependent torsion have been suggested by Van Rijn and Van den Berg (1993) in which $k = 1$ and Minken et al. (1995) in which $k = 1/2$. However, these models cannot account for the large variations in monocular torsion that occur during smooth asymmetric vergence; these variations include apparently random 'noise', systematic hysteresis, and idiosyncratic differences between subjects. In a binocular analysis cyclovergence does not show these variations, whereas cycloversion does.

A more accurate description of vergence-dependent torsion predicts cyclovergence $G = kev/2$ with $k = 1/2$. Thus a weak form of Listing's law seems to apply—binocular fixation determines cyclovergence. This torsion control strategy might support stereo vision by performing two useful functions. First, it governs the relative torsional alignment of the two eyes, preserving

stereo constancy. Second, it chooses the actual torsional alignment of each eye using some currently unknown criterion, such as optimising the placement of the vertical horopter (which seems unlikely) or aligning the horizontal retinal meridians. However, it is still not clear how or why the visual system tolerates such large, seemingly random variations in cycloversion.

Acknowledgements

Thanks to Michael Port for his help in constructing the apparatus described in this paper, and to Philip Duke (PD), Paul Warren (PW) and Sam Harrison (SH) for the use of their eyes. Thanks also to Chris Catherall for his help in collecting the data, to David Brennand for his orthoptic expertise, and to Paul Warren (again) for his mathematical assistance.

Appendix A. Torsion models and predictions

This Appendix summarises the mathematical models of vergence-dependent torsion with specific reference to the asymmetric vergence paradigm, and makes some predictions concerning the outcome of the experiment. The description assumes a left-handed co-ordinate frame with the centre of eye rotation as the origin.[6] For an excellent review of the co-ordinate systems used to describe eye movements see Haslwanter (1995).

A.1. Torsion models

An imaginary eye moving according to the Fick system would rotate horizontally about a stationary vertical axis, and then vertically about a mobile horizontal axis. One advantage of this arrangement is that the subjective vertical always remains parallel to the environmental vertical. However, to describe the radially symmetric rotational states of eye movements obeying Listing's law, the Fick system needs to be rotated about its optical axis; this apparent rotation of the eye with respect to the Fick vertical is sometimes called *false torsion*.

A.1.1. Fick torsion

Fick eye orientations are achieved by consecutive rotations through an angle g (gaze) about the y-axis and an angle e (elevation) about the x-axis. Rotation vector parameters E for elevation and G for gaze can be defined as follows:

$$E = \tan\frac{e}{2} \Leftrightarrow e = 2\ \tan^{-1} E$$

$$G = \tan\frac{g}{2} \Leftrightarrow g = 2\ \tan^{-1} G \tag{A.1}$$

These parameters can be used to specify Fick motion in rotation vector form for the left, l, and right, r, eyes:

$$l_{\text{Fick}} = \begin{pmatrix} 0 \\ G_{\text{L}} \\ 0 \end{pmatrix} \cdot \begin{pmatrix} -E_{\text{L}} \\ 0 \\ 0 \end{pmatrix} = \begin{pmatrix} -E_{\text{L}} \\ G_{\text{L}} \\ E_{\text{L}}G_{\text{L}} \end{pmatrix}$$

$$r_{\text{Fick}} = \begin{pmatrix} 0 \\ G_{\text{R}} \\ 0 \end{pmatrix} \cdot \begin{pmatrix} -E_{\text{R}} \\ 0 \\ 0 \end{pmatrix} = \begin{pmatrix} -E_{\text{R}} \\ G_{\text{R}} \\ E_{\text{R}}G_{\text{R}} \end{pmatrix} \tag{A.2}$$

Warren and Porrill (1996) showed that small angle approximations are entirely adequate to describe the state of the eyes in the asymmetric vergence task. If the angles for the viewing geometry shown in Fig. 2 are specified in radians then using a small angle approximation to the tangent function such that $\tan e/2 \approx e/2$ (and similarly for g) gives:

$$E_{\text{L}} \approx \frac{e}{2} \quad E_{\text{R}} \approx \frac{e}{2} \quad G_{\text{L}} \approx \frac{g_{\text{L}}}{2} = \frac{1}{2}(s+v)$$

$$G_{\text{R}} \approx \frac{g_{\text{R}}}{2} = \frac{1}{2}(s-v) \tag{A.3}$$

The gaze angles g_{L} and g_{R} for the two eyes can be decomposed into version s (half the sum) which is the same for both eyes, and vergence v (half the difference) which acts in different directions for the two eyes. (In the asymmetric vergence task the right is fixed horizontally such that $s - v = 0$.)

Substituting the approximations from Eq. (A.3) into Eq. (A.2) gives:

$$l_{\text{Fick}} \approx \begin{pmatrix} -e/2 \\ (s+v)/2 \\ e(s+v)/4 \end{pmatrix} \qquad r_{\text{Fick}} \approx \begin{pmatrix} -e/2 \\ 0 \\ 0 \end{pmatrix} \tag{A.4}$$

A.1.2. Listing torsion

By analogy with the Fick model (above), asymmetric vergence eye movements obeying Listing's law can be specified in rotation vector form as follows:

$$l_{\text{listing}} = \begin{pmatrix} -E_{\text{L}} \\ G_{\text{L}} \\ 0 \end{pmatrix} \approx \begin{pmatrix} -e/2 \\ (s+v)/2 \\ 0 \end{pmatrix}$$

$$r_{\text{listing}} = \begin{pmatrix} -E_{\text{R}} \\ G_{\text{R}} \\ 0 \end{pmatrix} \approx \begin{pmatrix} -e/2 \\ 0 \\ 0 \end{pmatrix} \tag{A.5}$$

[6] The x-axis joins the centres of eye rotation, and is a transverse line running from left to right; the y-axis is vertical, and positive upwards; the z-axis points straight ahead.

Note that both the gaze and elevation parameters have slightly different meanings in the Fick and Listing systems, though they coincide exactly for primary and secondary eye orientations, and approximately for non-eccentric tertiary eye orientations. In general, however, the values of E_L, G_L, E_R and G_R for Listing motion will differ from those for Fick motion.

Using small angle approximation, corresponding third entries in the rotation vectors can be subtracted to give the change in torsion between two states. Thus from Eq. (A.1), the angle of false torsion is approximately *twice* the difference between the third components of the Fick (Eq. (A.4)) and Listing (Eq. (A.5)) rotation vectors: $e(s+v)/2$ radians for the left eye and zero for the right eye.

A.1.3. Vergence-dependent torsion

The kinematic models proposed by Van Rijn and Van den Berg (1993) and Minken et al. (1995) both specify vergence-dependent torsion in terms of version, vergence and elevation as follows:

$$l_{\text{verg}} = \begin{pmatrix} -E_L \\ G_L \\ kE_L V \end{pmatrix} \approx \begin{pmatrix} -e/2 \\ (s+v)/2 \\ kev/4 \end{pmatrix}$$

$$r_{\text{verg}} = \begin{pmatrix} -E_R \\ G_R \\ -kE_R V \end{pmatrix} \approx \begin{pmatrix} -e/2 \\ 0 \\ -kev/4 \end{pmatrix} \quad \text{(A.6)}$$

The vergence parameter V is not related in a simple way to the angle v between the two fixation directions; however, for small angles the relationship $V \approx v/2$ holds.

Table 4
Torsion components during asymmetric vergence[a]

	Left eye	Right eye	Cyclo-version	Cyclo-vergence
Formula	L	R	(R+L)/2	(R−L)/2
Listing's (false) torsion	$ev/2$	0.00	$ev/4$	$-ev/4$
Vergence-dependent torsion	$kev/2$	$-kev/2$	0.00	$-kev/2$
Total change	$(k+1)ev/2$	$-kev/2$	$ev/4$	$-(2k-1)\times ev/4$
$k=1$	ev	$-ev/2$		$-3ev/4$
$k=1/2$	$3ev/4$	$-ev/4$		$-ev/2$

[a] This table shows predicted torsion angles during the asymmetric vergence task with the fixation target moving along the line-of-sight of the right eye. Note that predicted cycloversion does not depend on which model of vergence-dependent torsion is used.

A.2. Torsion predictions

The video-based eye-tracking system used in this experiment measures torsion relative to a Fick co-ordinate frame. Moving a fixation target along the line-of-sight of the right eye produces vergence changes in both eyes; however the change in the fixed right eye is offset by a change in version, so the eye does not rotate horizontally or vertically. Nevertheless, both eyes are expected to show vergence-dependent torsion; in addition, the left eye is expected to show torsion according to Listing's law. The observed left eye torsion L is therefore a combination of false torsion (Eqs. (A.4) and (A.5)) and vergence-dependent torsion (Eq. (A.6)); the corresponding right eye torsion R has no false component. The angles in this informal derivation are assumed to be small enough that the rotation vectors can simply be added, ignoring second-order effects:

$$L \approx \frac{es}{2} + \frac{(k+1)}{2} ev \qquad R \approx -\frac{k}{2} ev \quad \text{(A.7)}$$

The term $es/2$ is constant during the asymmetric vergence task, and so its contribution to torsion cannot be measured using the video system; however, the observed change in torsion is given by:

$$\Delta L \approx \frac{(k+1)}{2} ev \qquad \Delta R \approx -\frac{k}{2} ev \quad \text{(A.8)}$$

If $k=0$ then the observed change in torsion simply obeys Listing's law:

$$\Delta L = \frac{ev}{2} \qquad \Delta R = 0 \quad \text{(A.9)}$$

If $k=1$ as suggested by Van Rijn and Van den Berg (1993) then the observed torsion includes a vergence-dependent component in addition to, and of the same magnitude as, the false torsion:

$$\Delta L = ev \qquad \Delta R = -\frac{ev}{2} \quad \text{(A.10)}$$

If $k=1/2$ as suggested by Minken et al. (1995) then the vergence-dependent component is simply half that in the previous model, and the observed torsion change is:

$$\Delta L = \frac{3}{4} ev \qquad \Delta R = -\frac{ev}{4} \quad \text{(A.11)}$$

(Note that in the image frame the y-axis points downwards, so the signs are reversed—positive rotation in the image is therefore clockwise.)

Assuming a constant elevation angle e and changing vergence angle v formulae for the changes in monocular and binocular torsion are summarised in Table 4. The predicted Listing and vergence-dependent components are added together to give the overall predicted torsion for the left eye; the torsion for the right eye is simply the vergence-dependent component with opposite sign.

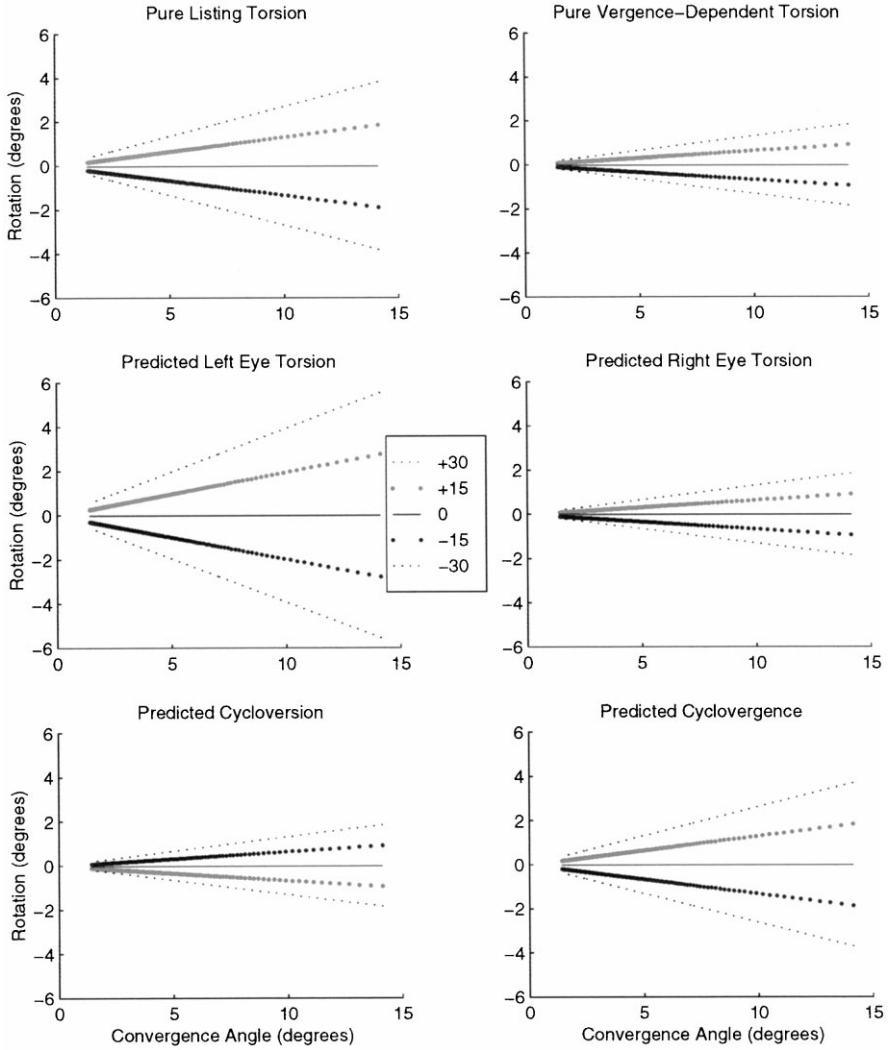

Fig. 10. Predicted monocular and binocular torsion. These graphs show the predicted torsion for the asymmetric vergence task with the right eye fixed at five different elevations. The topleft graph shows the torsion predicted by Listing's law (which only applies for the mobile left eye). The topright graph shows the vergence-dependent torsion predicted using the kinematic model with $k = 1/2$ (if $k = 1$ then the resulting graph is identical to that for Listing's law). The remaining graphs show the monocular and binocular torsion produced by combining these components.

Fig. 10 shows the torsion predicted for the asymmetric vergence task using the formulae in Table 4; these graphs are included for direct comparison with the results in Figs. 4–7.

A.3. Note on approximations

For simplicity, the elevations of the left and the right eyes are assumed to be the equal in the asymmetric vergence task (see Eqs. (A.3), (A.4) and (A.5)). However, in a Fick co-ordinate system the elevations of the two eyes are only the same during symmetric binocular fixation. During asymmetric fixation the elevation of the left eye is always smaller in magnitude than that of the right eye, especially for short fixation distances.

The approximation signs in the formulae in this Appendix indicate that only the lowest-order (largest) term in each vector component was retained. Thus, although the elevation of the left eye does vary slightly, the resulting dependence of elevation on vergence does not appear in the formulae. Nevertheless, the single term retained is sufficient to calculate the lowest-order contribution to torsion correctly. The adequacy of these approximations was carefully checked by numerical simulation during preliminary work on the experiment—see Warren and Porrill (1996).[7] Errors in calcu-

[7] There appears to be a distrust of approximations in the vision literature, which often results in overlong derivations of unwieldy, uninformative, and sometimes incorrect formulae. (This contrasts with the ubiquitous use of approximate formulae in the physical sciences.) In those (relatively few) instances in which more accurate values are required than can be recovered from simple approximations (for example to check accuracy) they can usually be obtained numerically far more reliably and with less effort than by using exact formulae.

lating torsion were found to be roughly proportional to elevation, with a maximum error of about 0.05° for asymmetric vergence at 30° elevation. The slight change in left eye elevation during the asymmetric vergence task is thus at least an order of magnitude smaller than necessary to corrupt the torsion measurements or predictions. Since the approximations are adequate, they are used in preference to unwieldy exact formulae which are difficult to derive and would not add much to the interpretation of the data. Consequently, all of the graphs that depend on elevation quote the (constant) Fick elevation of the right eye.

References

Bruno, P., & Van den Berg, A. V. (1997). Relative orientation of primary positions of the two eyes. *Vision Research*, *37*, 935–947.

Enright, J. T. (1990). Stereopsis, cyclotorsional noise and the apparent vertical. *Vision Research*, *30*(10), 1487–1497.

Haslwanter, T. (1995). Mathematics of three-dimensional eye rotations. *Vision Research*, *35*(12), 1727–1739.

Helmholtz von, H. (1867). *Handbuch der Physiologischen Optik* (1st ed.). Hamburg: Voss (J. P. C. Southall, Trans.: Third edition translated into English as Helmholtz's treatise on physiological optics. New York: Optical Society of America).

Hepp, K. (1990). On Listing's law. *Communications in Mathematical Physics*, *132*, 285–292.

Hering, E. (1868). *The theory of binocular vision*. New York: Plenum Press (B. Bridgeman, L. Stark, Trans.; 1977).

Ivins, J., Porrill, J., & Frisby, J. (1998). A deformable model of the human iris for measuring ocular torsion from video images. *IEEE Proceedings on Vision, Image and Signal Processing*, *145*(3) (pp. 213–220).

Ivins, J., Porrill, J., & Frisby, J. (1999). Instability of torsion during smooth asymmetric vergence. *Vision Research*, *39*, 993–1009.

Minken, A. W. H., Gielen, C. C. A. M., & Van Gisbergen, J. A. M. (1995). An alternative 3D interpretation of Hering's equal-innervation law for version and vergence eye movements. *Vision Research*, *35*, 93–102.

Mok, D., Ro, A., Cadera, W., Crawford, J. D., & Vilis, T. (1992). Rotation of Listing's plane during vergence. *Vision Research*, *32*, 2055–2064.

Moore, S. T., Haslwanter, T., Curthoys, I. S., & Smith, S. T. (1996). A geometric basis for measurement of three dimensional eye position using image processing. *Vision Research*, *36*, 445–459.

Nakayama, K. (1983). Kinematics of normal and strabismic eyes. In C. M. Schur, & K. J. Ciuffreda, *Vergence eye movements: basic and clinical aspects* (pp. 543–564). Boston, MA: Butterworths.

Tweed, D. (1997). Visual-motor optimisation in binocular control. *Vision Research*, *37*(14), 1939–1951.

Tyler, C. W. (1983). Sensory processing of binocular disparity. In C. M. Schur, & K. J. Ciuffreda, *Vergence eye movements: basic and clinical aspects* (pp. 199–295). Boston, MA: Butterworths.

Warren, P., & Porrill, J. (1996). *Eyelab*: *mathematical predictions of the dependence of torsion on vergence*. AIVRU memo no. 115, Department of Psychology, University of Sheffield.

Van Rijn, L. J., & Van den Berg, A. V. (1993). Binocular eye orientation during fixations: Listing's law extended to include eye vergence. *Vision Research*, *33*(5/6), 691–708.